POLITECNICO DI TORINO
Repository ISTITUZIONALE

Fully automated quantitative assessment of hepatic steatosis in liver transplants

Availability:
This version is available at: 11583/2837874 since: 2020-07-02T11:13:23Z

Publisher:
Elsevier

Published
DOI:10.1016/j.compbiomed.2020.103836

Terms of use:

This article is made available under terms and conditions as specified in the corresponding bibliographic description in the repository

(Article begins on next page)

01 May 2024

Fully automated quantitative assessment of hepatic steatosis in liver transplants

Massimo Salvi[a,*] massimo.salvi@polito.it, Luca Molinaro[b], Jasna Metovic[c], Damiano Patrono[d], Renato Romagnoli[d], Mauro Papotti[c], Filippo Molinari[a]

[a]Politobiomed Lab, Biolab, Department of Electronics and Telecommunications, Politecnico di Torino, Turin, Italy

[b]Division of Pathology, AOU Città Della Salute e Della Scienza di Torino, Turin, Italy

[c]Division of Pathology, Department of Oncology, University of Turin, Turin, Italy

[d]General Surgery 2U, Liver Transplant Center, AOU Città Della Salute e Della Scienza di Torino, University of Turin, Turin, Italy

[*]Corresponding author. Biolab, Department of Electronics and Telecommunications, Politecnico di Torino, Torino, Italy.

Abstract

Background: The presence of macro- and microvesicular steatosis is one of the major risk factors for liver transplantation. An accurate assessment of the steatosis percentage is crucial for determining liver graft transplantability, which is currently based on the pathologists' visual evaluations on liver histology specimens.

Method: The aim of this study was to develop and validate a fully automated algorithm, called HEPASS (HEPatic Adaptive Steatosis Segmentation), for both micro- and macro-steatosis detection in digital liver histological images. The proposed method employs a hybrid deep learning framework, combining the accuracy of an adaptive threshold with the semantic segmentation of a deep convolutional neural network. Starting from all white regions, the HEPASS algorithm was able to detect lipid droplets and classify them into micro- or macrosteatosis.

Results: The proposed method was developed and tested on 385 hematoxylin and eosin (H&E) stained images coming from 77 liver donors. Automated results were compared with manual annotations and nine state-of-the-art techniques designed for steatosis segmentation. In the TEST set, the algorithm was characterized by 97.27% accuracy in steatosis quantification (average error 1.07%, maximum average error 5.62%) and outperformed all the compared methods.

Conclusions: To the best of our knowledge, the proposed algorithm is the first fully automated algorithm for the assessment of both micro- and macrosteatosis in H&E stained liver tissue images. Being very fast (average computational time 0.72 s), this algorithm paves the way for automated, quantitative and real-time liver graft assessments.

1 Introduction

Liver transplantation (LT) is a standard treatment in patients with end-stage liver disease (ESLD) and hepatocellular carcinoma [1]. In the United States, nearly 7000 liver transplants are performed each year [2]. LT procedure entails multidisciplinary teamwork of different healthcare professionals including the pathologist, who plays a key role during pre- and post-transplantation liver graft assessment. Liver biopsy is still considered the gold standard for pre- and post-transplant graft evaluation [3,4]. In the donor setting, accurate evaluation of histological prognostic parameters, such as necrosis, macro- and microvesicular steatosis has an important role in assessing the suitability for transplant of a particular graft and in stratifying the risk associated with its utilization.

In organ transplantation, one major challenge is trying to close the ever-increasing gap between increasing demand and organ availability. This has pushed transplant clinicians to several attempts at expanding donor pool, including the utilization of grafts from extended criteria donors (ECD) [5–9]. Although definition of what is a suboptimal graft is still arbitrary, it is well known that graft steatosis is associated with postoperative graft dysfunction and reduced patient and graft survival [10–13]. There are two forms of steatosis diagnosed in liver grafts: macrovesicular steatosis, in which lipids are stored in a single large vesicle occupying almost the entire hepatocyte cytoplasm, is generally associated with excessive alcohol intake, obesity, hyperlipidemia and diabetes; microvesicular steatosis, which is characterized by smaller vacuoles, is commonly observed in pathological conditions related to mitochondrial injury, such as acute viral or drug induced injury, sepsis and some metabolic disorders [14,15]. Moderate (>30%) macrovesicular steatosis has been frequently associated with inferior outcomes after LT [16], whereas even marked microvesicular steatosis has not been associated with poorer graft function [17], highlighting that accurate distinction of macro- and microvesicular steatosis is of paramount importance during graft assessment. However, also outcome of utilization of grafts with moderate or severe (>60%) macrovesicular steatosis varies widely in the literature. For example, the rate of 1-year graft failure in presence of severe macrovesicular steatosis ranges from 5.3% to 75% [14,16,18,19].

These extremely variable findings are at least partially explained by the inherent limitations of steatosis assessment. The traditional evaluation of hepatic steatosis involves significantly subjective, complex and time-consuming microscopic evaluation, with low concordance levels among observers. Histological assessment is typically qualitative, including a description of the size of fat droplets and their location within the lobule, or semiquantitative, with a subjective multigrade scale based on the proportion of hepatocytes with steatotic droplets [20]. Thus, this score is subjected to inter-observer and intra-observer variability and is prone to inaccuracy [21,22].

The necessity to overcome these limitations has prompted the development of digital image analysis methods for unbiased and reproducible steatosis assessments of Hematoxylin and Eosin (H&E) stained liver slides. Considering the above-mentioned data and complex background, a digital image analysis method was developed for unbiased and reproducible steatosis assessments of H&E-stained liver slides.

Current research focuses on the development of fully automated methods for quantitative histological analysis, in order to create accurate tools with high reproducibility [23–25]. These approaches can provide a continuous measure for analysis and reduce inter- and intra-observer variability in the measurement of cellular structures, increasing the reproducibility of the results [26]. In the last few years, several automated methods were proposed

for quantitative assessment of liver steatosis [27–29]. Different approaches have been used to automatically detect steatosis from the histological tissue, ranging from tools using simply thresholding [30,31] to algorithms incorporating several features, with predetermined cut-offs [32,33] and recently more advanced approaches such as supervised machine learning [34,35]. Catta-Preta et al. [29] proposed white thresholding without any post-processing step. Turlin et al. [30] and Liquori et al. [31] employed a fixed threshold followed by morphological filters to detect liver steatosis. Nativ et al. [33] applied an iterative active contour to obtain the boundaries of liver droplets. Batool et al. [27] and Vanderbeck et al. [28] took advantage of the green channel of RGB image to apply global thresholding. Then, non-circular binary shapes were deleted from the final mask. Tsiplakidou et al. [32] proposed two-stage processing. In the first stage, histogram equalization and image binarization were applied while the second stage consisted of eccentricity and roundness criteria. Recent methods combined iterative morphological operators with shape and texture features to classify regions in steatosis and non-steatosis [35]. Munsterman et al. [34] applied two thresholds in the saturation channel of the HSB color representation and employed a logistic regression analysis to detect all the fat droplets. Nonetheless, these algorithms apply simple fixed threshold, do not discriminate between micro- and macro-vesicular steatosis (fundamental for a correct prognosis estimate) and they still include some manual interventions (e.g. visual examination to exclude false-positive shapes). In addition, datasets, manual annotations and source codes of previously published methods are not publicly available.

In this paper, a novel steatosis segmentation strategy for histopathological images is presented. The proposed method employs a hybrid deep learning framework, combining the accuracy of an adaptive threshold with the semantic segmentation of a deep convolutional neural network. The aim of the present study was to (i) develop a fully automated steatosis quantification algorithm for both micro- and macro steatosis; (ii) compare the automatic results with manual pathologist evaluation and (iii) compare the performance of our method with the current state-of-art techniques.

2 Materials and methods

In this paper, an automated method called HEPASS (HEPatic Adaptive Steatosis Segmentation) is presented. The HEPASS algorithm is an automatic and adaptive method for liver steatosis quantification in H&E stained images. The flowchart of the proposed method is shown in Fig. 1. The algorithm consists of four modules: histological tissue detection, raw steatosis segmentation, extended steatosis detection and cleaning steps. In the following sections, a detailed description of the algorithm is provided.

alt-text: Fig. 1

Fig. 1

Figure Replacement Requested
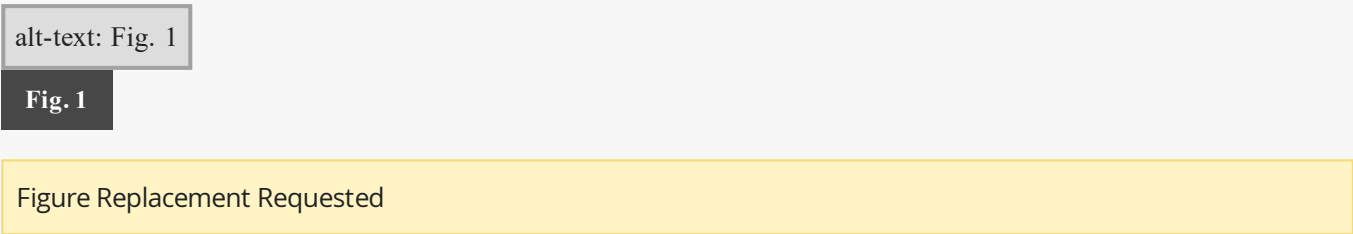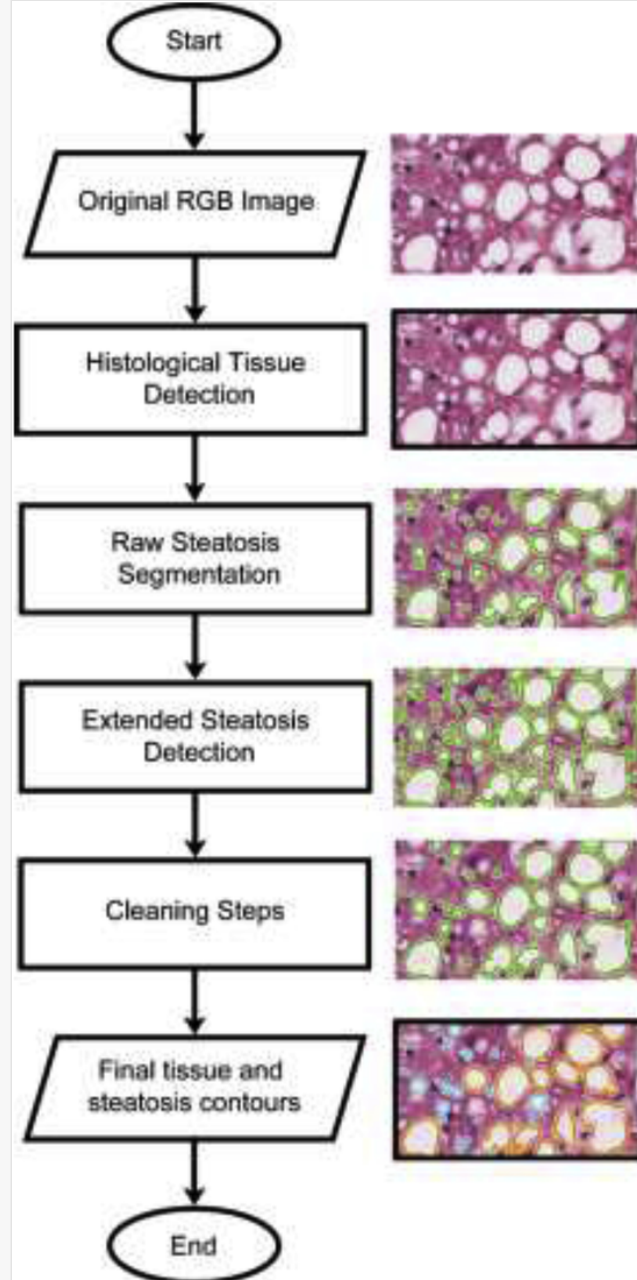
Schematic representation of the HEPASS algorithm. Starting from the RGB image, the histological tissue contours are automatically detected. A first segmentation of liver steatosis is obtained by the 'Raw Steatosis Segmentation' step. Then, the algorithm detects all the candidate steatosis ('Extended Steatosis Detection'). Finally, several cleaning steps are applied to obtain the final segmentation of the hepatic steatoses within the image.

Replacement Image: Figure 1.tif

Replacement Instruction: High-quality figure

2.1 Human liver histology

The consecutive liver biopsy specimens of 77 patients (males 55, females 23; median age 54.5 years, range 1–68 years) obtained from January 1st to December 31st, 2017 were collected. Liver biopsies were obtained during organ retrieval or at the end of transplant operation at Città della Salute e della Scienza Hospital in Turin, Italy. The tissues were collected by core needle biopsy, formalin-fixed and paraffin-embedded, serially sectioned to 5 μm, mounted onto adhesive slides, and stained with conventional H&E coloration. Routine H&E staining was performed, following standard procedures (Leica ASP 300 processor and automated Leica ST5020 Multistainer, Leica Microsystems, Wetzlar, Germany). All biopsy samples were collected at the Division of Pathology, AOU Città della Salute e della Scienza Hospital, Turin, Italy and were anonymized by a pathology staff member not involved in the study, before any further analysis was started. Digital images were obtained with a Hamamatsu NanoZoomer S210 Digital slide scanner providing a magnification of ×200 (conversion factor: 0.467 μm/pixel). Five images with a fixed dimension of 416 × 416 pixels were randomly extracted from each biopsy, for a total of 385 images. After consensus, manual annotations of hepatic steatosis contours were generated by two of us (LM and JM), for a total of 12929 shapes. The overall dataset composition is shown in Table 1. The image dataset, along with the manual annotations used in this work, are available at https://data.mendeley.com/datasets/4mcc9rg4k5/[Instruction: To DC: We published our repository. The updated link is:
https://data.mendeley.com/datasets/4mcc9rg4k5/1
Kindly link]1.

alt-text: Table 1

Table 1

> (i) The table layout displayed in this section is not how it will appear in the final version. The representation below is solely purposed for providing corrections to the table. To preview the actual presentation of the table, please view the Proof.

Dataset composition.

Dataset	#Patients	#Images	#Annotations
TRAIN	70	350	11567
TEST	7	35	1362

https://data.mendeley.com/datasets/4mcc9rg4k5/draft?a=beff0dba-6534-4475-9849-1b25422f38a1.https://data.mendeley.com/datasets/4mcc9rg4k5/1

2.2 Histological tissue detection

Starting from the original RGB image of the specimen (Fig. 2a), the HEPASS algorithm performed the discrimination between the histological tissue and the background. The aim of this step was to process only the cellular structures within the image. The tissue recognition occurred thanks to the application of an RGB high-pass filter [36] where the RGB color of each pixel was treated as a 3D vector, and the strength of the edge was the magnitude of the maximum gradient. Then, Otsu thresholding [37] was applied to extract a raw binary mask of the tissue and a morphological opening with a disk of 3-pixel radius (equal to 1.40 μm) is carried out to obtain smoother tissue contours (Fig. 2b).

Figure Replacement Requested
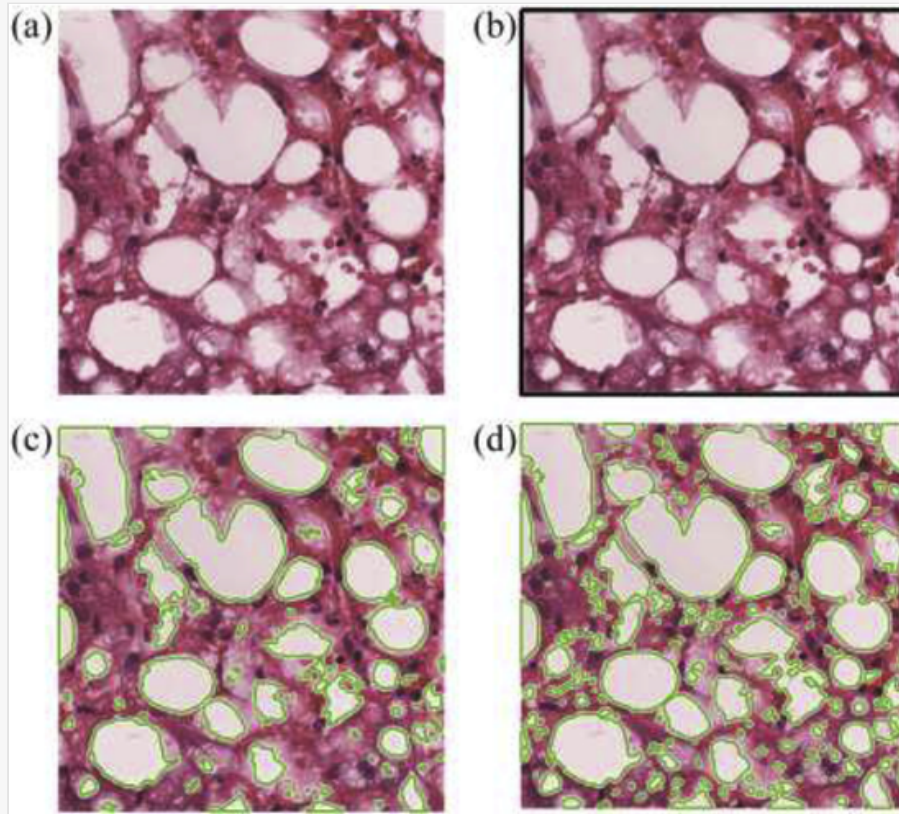
Initial steatosis detection of the HEPASS algorithm. (a) Original image, (b) histological tissue segmentation, (c) raw steatosis segmentation, (d) extended steatosis detection.

2.3 Raw steatosis segmentation

Once obtained the tissue boundary, the algorithm performed a first steatosis segmentation. Simple thresholding may be ineffective to segment liver steatosis, since they often have different intensity and uniformity depending on their size, shape, and the presence of artefacts. Therefore, in order to properly segment the steatosis, a series of Gabor kernels were applied to the original grayscale image. The kernels were defined as follows:

$$g(x, y, \lambda, \theta, \psi, \sigma, \gamma) = exp\left(\frac{-x'^2 + \gamma^2 y'^2}{2\sigma^2}\right) cos\left(\frac{2\pi x'}{\lambda} + \psi\right)$$

(1)

where $x' = x\cos(\theta) + y\sin(\theta)$, $y' = -x\sin(\theta) + y\cos(\theta)$, γ is the spatial aspect ratio that specifies the ellipticity of the Gabor function, ψ represents the phase offset, λ is the wavelength of the sinusoidal factor, θ denotes the orientation of the normal to the parallel stripes of a Gabor function and σ is the standard deviation of the Gaussian envelope. For this application, we imposed $\gamma = 1.2$, $\psi = 0$, $\lambda = 10$, $\sigma = 1$ and eight directions (θ) were considered to make the algorithm faster and to still reduce the noise level. The obtained eight filtered images

were summed and normalized; then a threshold equal to 90% of the image maximum was applied. Finally, the proposed method applied an active contour model to improve the detection of steatosis borders [38], as shown in Fig. 2c.

2.4 Extended steatosis detection

Since some small or not completely white structures may not be identified using a fixed threshold, an adaptive two-step refining process was applied to better define all the liver steatosis:

1. *Optimized thresholding*: histological slides are often affected by stain intensity variability, therefore a fixed threshold could not guarantee optimal performance. An adaptive color deconvolution developed in our previous work [39] was applied to obtain the separation between Hematoxylin and Eosin channels. Then, the estimated RGB color of the Eosin was converted in grayscale and an optimal threshold equal to $\left(\text{Eosin} + \frac{40}{255} \right)$ was applied. In this way, it was possible to adapt the threshold based on the stroma intensity.

2. *Active contour model*: starting from the binary mask obtained at the previous step, the Chan-Vese region-based energy model [40] was applied to detect microsteatosis. Thanks to this model, it was possible to detect objects whose boundaries are not necessarily defined by gradients.

At the end of these steps, the steatosis binary mask was merged with the one of the previous section ('Raw Steatosis Segmentation'), obtaining the result shown in Fig. 2d.
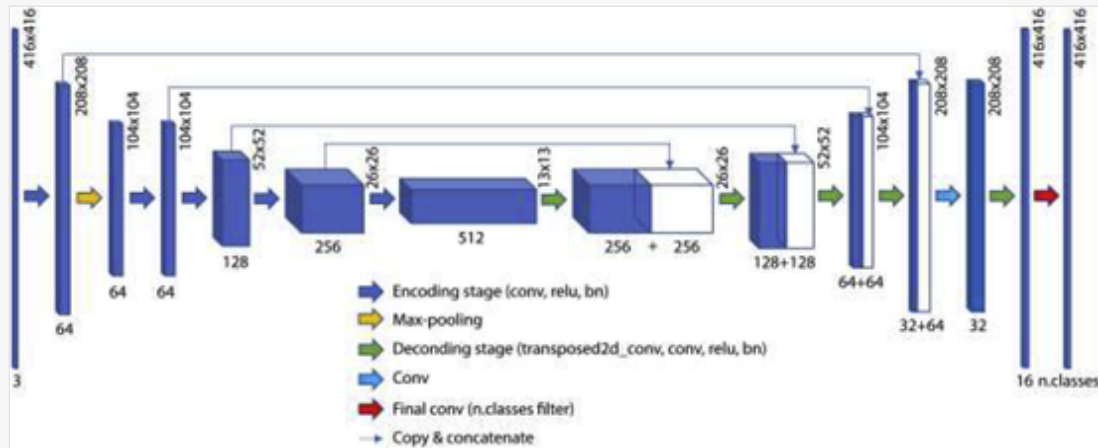
2.5 Cleaning steps

At this point, the proposed method was able to extract a set of potential steatotic hepatocytes within the image. However, the resulting binary mask contained erroneous white regions due to pathological cell ballooning, anatomical tracts, tissue damage, and empty slide background as well in addition to liver steatosis. For this reason, the HEPASS algorithm applied a series of cleaning steps to distinguish steatosis from not-of-interest objects (e.g. bile ducts, sinusoid, blood vessels and tissue tearing) based on size and roundness features. Preliminarily, detected objects with area less than 10 μm^2 were deleted because they were too small to be considered as steatosis. Then, the blobs corresponding to lipids were divided into macro steatosis (area >175 μm^2) and micro steatosis (area ≤175 μm^2) according to Liquori et al. [31]. Finally, the algorithm applied two different cleaning criteria for macro- and microsteatosis, as follows.

In order to distinguish between macro steatosis and other white structures, we integrated a deep convolutional neural network (CNN) within our pipeline. A U-Net network with ResNet34 backbone was implemented to perform semantic segmentation (Fig. 3). This network consisted of an encoder and a decoder structure. The encoder network, based on the ResNet34 architecture, was designed to extract high-level features from the input image. The decoder network aimed to semantically project the discriminating characteristics (lower resolution) learned by the encoder on the pixel space (higher resolution) to obtain a dense classification [41]. Our deep convolutional network was based on residual blocks, which consisted of a sequence of layers with skip connections between input and output of each block [41]. The encoding part of our network was pre-trained on the 2012 ILSVRC imageNet Dataset [42]. Then, the entire network was trained using the 350 RGB images of the TRAIN dataset.

alt-text: Q2: Please note that author's telephone/fax numbers are not published in Journal articles due to the fact that

articles are available online and in print for many years, whereas telephone/fax numbers are changeable and therefore not reliable in the long term.Fig. 3

Fig. 3

Figure Replacement Requested

Architecture of the deep network employed to perform macro-steatosis segmentation. A U-Net with ResNet34 backbone was implemented using Keras framework.

Replacement Image: Figure 3.tif

Replacement Instruction: High-quality images

Starting from the original image, the deep network was employed to detect liver steatosis (Fig. 4a). We adopted the semantic segmentation to reject false positive shapes from the candidate macro steatosis mask (Fig. 2d). In particular, all the regions not detected by CNN were removed from the extended steatosis mask, thus obtaining the result shown in Fig. 4b. However, as can be seen from Fig. 4b, the steatosis segmentation was not accurate as lipid droplets were merged together. For this reason, the HEPASS algorithm performed a separation of the detected regions using an active deformable model. This step was necessary to correct the over-segmentation of the previous step since too large structures may consist of a fusion of several steatosis vacuoles. The distance transform of the binary mask was computed, and its local maxima were extracted to initialize the deformable model. In each local maximum, a 'balloon' active contour [43] was then initialized with the following energy function (E):

$$E = \alpha \cdot \vec{n}(s) + \beta \cdot \left| \frac{dv}{ds} \right|^2 + \gamma \cdot |\nabla I_K|^2$$

(3)

where $v(s)$ was the parametric form of the curve, α regulated the radial expansion, $\vec{n}(s)$ was the normal unity vector of the curve, β was the coefficient related to the elasticity of the curve, while γ and ∇I_K were the external energy's coefficient and the Sobel gradient of the grayscale image, respectively. For this application, we set $\alpha = 0.15$, $\beta = 0.05$ and $\gamma = 1.2$. A number of points equal to 100 was used for each active contour. The result obtained by the active deformable model is shown in Fig. 4c.

alt-text: Fig. 4

Fig. 4

Figure Replacement Requested
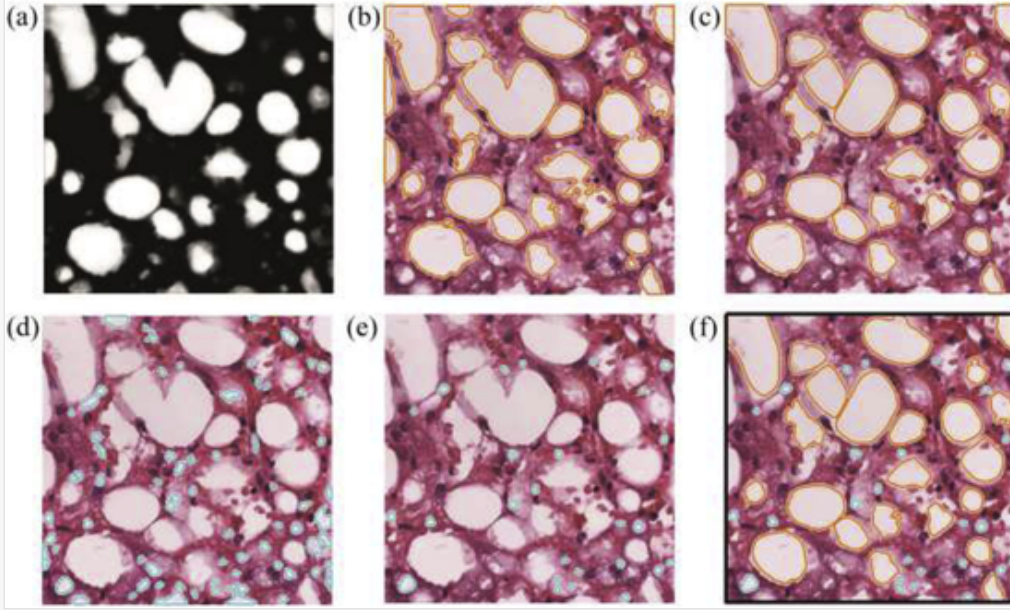
Cleaning steps of the HEPASS algorithm. (a) Output of the CNN designed for steatosis segmentation, (b) initial macro steatosis mask (orange), (c) active contour model for structure separation, (d) initial micro steatosis mask (cyan), (e) cleaning of micro steatosis using logistic regression, (f) final result of the proposed algorithm. ~~(For interpretation of the references to color in this figure legend, the reader is referred to the Web version of this article.)~~

Replacement Image: Figure 4.tif

Replacement Instruction: High-quality image

To perform the separation between true microsteatosis (area ≤ 175 μm^2) and the other objects with the same size, the statistical classifier based on logistic regression analysis proposed by Munsterman et al. [34] was implemented. Briefly, this classifier used measures expressing the roundness of objects, using quantitative features as *size* (μm^2), *circularity, roundness* and *solidity*. These four features were used to detect microsteatosis since they ensure the best performance compared to other morphological and chromatic characteristics [34]. For each detected microstructure (Fig. 4d), the following classifier was employed:

$$Pr(\cdot) = \frac{10^{logit}}{10^{logit} + 1}$$

(4)

where logit (.) was the result of the logistic regression analysis:

$$logit = -16.2 + 0.00272 \times size + 4.81 \times circularity + 6.054 \times roundness + 9.3 \times solidity$$

(5)

All the microstructures that achieved a probability (Pr) lower than 95% were deleted. The result obtained after applying this cleaning step is illustrated in Fig. 4e.

At the end of the processing, the summed surface area of all detected steatosis as well as the total tissue area was calculated. The automatic result provided by the HEPASS algorithm is shown in Fig. 4f. Finally, the algorithm

computed the SPA (steatosis proportionate area) as:

$$SPA = \frac{\sum steatosis_{area}}{\sum tissue_{area}}$$

(6)

2.6 Performance measure

A comparison between masks drawn by a manual operator and those provided by our method was carried out to assess the algorithm performance in the segmentation of histological tissue and hepatic steatosis. Firstly, the segmentation accuracy was computed as:

$$accuracy = \frac{TP + TN}{TP + TN + FP + FN}$$

(7)

where TP: true positive, TN: true negative, FN: false negative and FP: false positive. Besides pixel-based results, the absolute error (AE) between manual and automatic steatosis percentage (SPA) was also evaluated. In order to perform a quantitative assessment of the histological image, we compared the mean area of manually detected regions with automatic ones. For each image, the error between manual and automatic estimation was calculated as:

$$error_{regions} = \frac{\sum_{i=1}^{N} area_{manual}(i)}{N} - \frac{\sum_{j=1}^{M} area_{automatic}(j)}{M}$$

(8)

where N and M are the number of regions manually and automatically detected, respectively. Finally, the classification accuracy of the automated method in steatosis quantification (SQ) was evaluated.

3 Results

The automatic results provided by the HEPASS algorithm were compared both with manual steatosis annotations and previously published works. For the implementation of each published algorithm, we followed the pipeline described within the respective 'Materials and Methods' section. For all the state-of-art methods, a quantitative comparison was carried out by evaluating the accuracy in the segmentation of the histological tissue (accuracy$_{TISSUE}$) and liver steatosis (accuracy$_{STEATOSIS}$). Table 2 shows the comparison between the proposed algorithm and the current state-of-art methods. The HEPASS algorithm exhibited excellent performances in segmenting hepatic steatosis; the very high average accuracy coupled to low standard deviation values demonstrated the robustness of the method. In both TRAIN and TEST datasets, the proposed strategy outperformed compared methods, obtaining an average accuracy$_{STEATOSIS}$ of 97.53% and 97.27%, respectively. Correspondingly, the visual performances of the compared methods are reported in Fig. 5. The HEPASS algorithm was able to correctly detect and separate the macro-steatosis fused together (Fig. 5 – Sample #1). Thanks to the semantic segmentation of the deep network, our method was also capable to avoid the detection of false-positive shapes in images with a high concentration of sinusoids (Sample #3).

alt-text: Table 2

Comparison between the proposed algorithm and the state-of-art methods during histological tissue and liver steatosis segmentation. Accuracy $_{TISSUE}$ and accuracy $_{STEATOSIS}$ indicates the accuracy in tissue and steatosis detection, respectively.

Method	TRAIN		TEST	
	accuracy $_{TISSUE}$ (%)	accuracy $_{STEATOSIS}$ (%)	accuracy $_{TISSUE}$ (%)	accuracy $_{STEATOSIS}$ (%)
Turlin et al.	83.10 ± 26.64	96.94 ± 6.49	82.59 ± 27.61	96.00 ± 7.76
Liquori et al.	83.10 ± 26.64	96.05 ± 6.67	82.59 ± 27.61	95.01 ± 9.10
Catta-Preta et al.	98.40 ± 3.50	91.60 ± 8.61	97.83 ± 4.12	91.33 ± 8.51
Nativ et al.	83.10 ± 26.64	95.77 ± 4.91	82.59 ± 27.61	95.47 ± 5.17
Vanderbeck et al.	97.54 ± 6.33	96.51 ± 3.71	96.73 ± 5.95	96.04 ± 5.14
Batool et al.	95.22 ± 11.97	96.49 ± 5.10	94.45 ± 12.31	95.97 ± 6.90
Tsiplakidou et al.	83.10 ± 26.64	97.02 ± 5.23	82.59 ± 27.61	95.76 ± 8.03
Arjmand et al.	87.34 ± 25.72	96.37 ± 5.76	86.81 ± 27.62	94.93 ± 8.62
Munsterman et al.	95.50 ± 10.89	96.66 ± 4.79	97.70 ± 4.54	95.68 ± 7.71
HEPASS algorithm	**99.08 ± 1.34**	**97.53 ± 2.37**	**99.30 ± 0.93**	**97.27 ± 2.71**

alt-text: Fig. 5

Fig. 5

Figure Replacement Requested
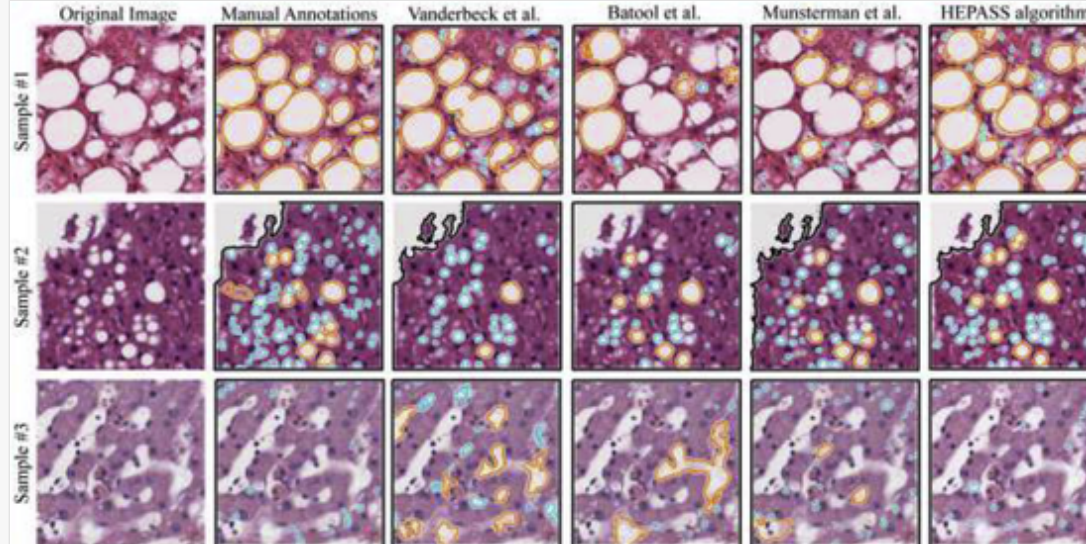
Visual performance between the best three published methods for steatosis detection and the proposed algorithm. Sub-images from different samples are shown in rows while segmentation results are illustrated in columns. First column displays the original image while manual annotations generated after consensus of two expert pathologists are illustrated in the second column. Compared methods are presented from the third column while the result of the HEPASS algorithm is shown in the last one.

Replacement Image: Figure 5.tif

Replacement Instruction: High-quality image

Once obtained the tissue and steatosis contours, we also evaluated the absolute errors between manual and automatic SPA (steatosis proportionate area). Table 3 illustrates the absolute errors (AE) between manual and automatic steatosis percentage. In both TRAIN and TEST datasets, the HEPASS algorithm achieved the lowest average AE (0.95% and 1.07%), with a maximum AE of 5.55% and 5.62%, respectively. Specifically, the maximum AE obtained by the algorithm was 4–10 times lower compared to state-of-art techniques. Fig. 6 shows the absolute errors during SPA evaluation for all the hepatic steatosis and for the macrovesicular and microvesicular ones. Our algorithm obtained the best performance in SPA evaluation for both micro- and macrosteatosis, with a mean value of 0.51% and 0.66%, respectively. In addition to being accurate, the proposed method is also fast, with an average computational time of 0.72 s.

alt-text: Table 3

Table 3

The table layout displayed in this section is not how it will appear in the final version. The representation below is

Minimum, average and maximum absolute errors (AE_{MIN}, AE_{MEAN}, AE_{MAX}) between manual and automatic steatosis percentage for both TRAIN and TEST datasets.

Method	TRAIN			TEST		
	AE_{MIN} (%)	AE_{MEAN} (%)	AE_{MAX} (%)	AE_{MIN} (%)	AE_{MEAN} (%)	AE_{MAX} (%)
Turlin et al.	0	3.37	88.72	0	4.34	41.68
Liquori et al.	0	4.51	52.78	0	5.48	42.75
Catta-Preta et al.	0.03	4.74	40.51	0.05	5.71	32.82
Nativ et al.	0	3.58	33.05	0.04	3.68	16.91
Vanderbeck et al.	0.01	2.55	18.42	0.03	3.23	16.28
Batool et al.	0	2.93	39.86	0.01	3.39	32.29
Tsiplakidou et al.	0	3.16	49.61	0	4.33	39.43
Arjmand et al.	0	2.63	46.45	0.07	3.87	35.80
Munsterman et al.	0	1.85	42.41	0	2.64	36.35
HEPASS algorithm	**0**	**0.95**	**5.55**	**0**	**1.07**	**5.62**

alt-text: Fig. 6

Fig. 6

Figure Replacement Requested
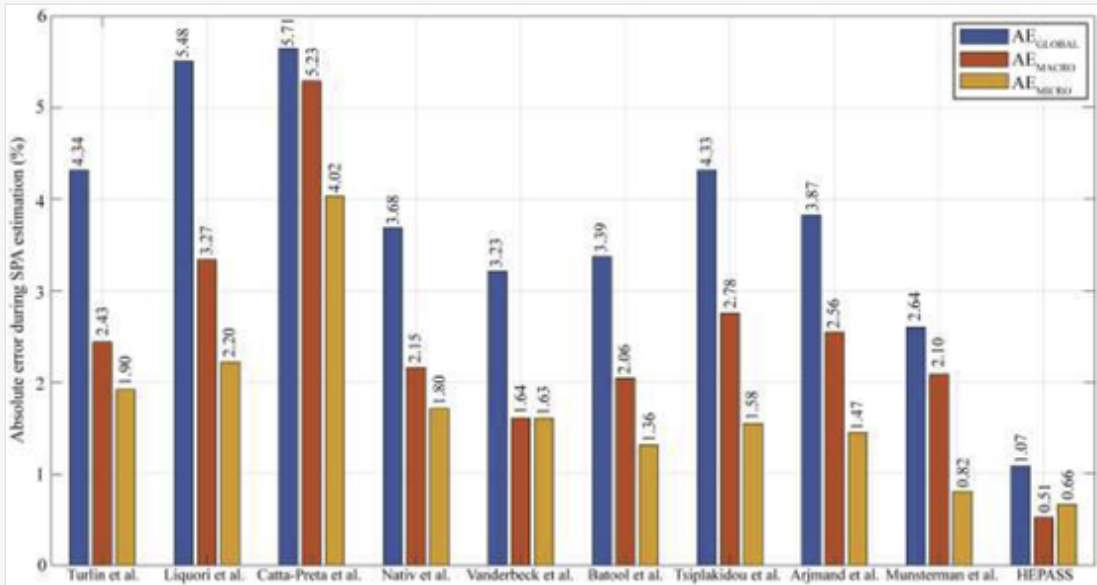
Quantitative comparison between the HEPASS algorithm and the state-of-art methods during SPA calculation for the TEST dataset. AE_{GLOBAL} indicates the absolute error for all the hepatic steatosis while AE_{MACRO} and AE_{MICRO} represent the absolute errors for the macrovesicular and microvesicular steatosis, respectively.

Finally, we computed the average error between manual and automatic steatosis area (error$_{REGIONS}$) and the classification accuracy of the automated methods using SQ system (Table 4). Also in this case, the proposed technique outperformed the compared methods, obtaining the lowest error$_{REGIONS}$ (3.65 μm^2) and the highest classification accuracy using SQ system (97.14%) in the TEST set.

alt-text: Table 4

Table 4

> ⓘ The table layout displayed in this section is not how it will appear in the final version. The representation below is solely purposed for providing corrections to the table. To preview the actual presentation of the table, please view the Proof.

Average error between the area of manually annotated steatosis and automatically detected ones (error$_{REGIONS}$) and classification accuracy of the automated methods using SQ system.

Method	TRAIN		TEST	
	error$_{REGIONS}$ (μm^2)	SQ$_{ACCURACY}$ (%)	error$_{REGIONS}$ (μm^2)	SQ$_{ACCURACY}$ (%)
Turlin et al.	−170.40	78.57	−43.94	82.86
Liquori et al.	36.07	71.14	49.46	71.43
Catta-Preta et al.	−27.77	51.43	4.31	45.71
Nativ et al.	−74.75	73.43	−47.47	68.57
Vanderbeck et al.	−263.00	80.57	−515.20	80.00
Batool et al.	25.53	79.14	34.66	82.86
Tsiplakidou et al.	−23.08	80.00	−5.68	82.86
Arjmand et al.	−26.60	82.86	−4.56	77.14
Munsterman et al.	18.19	91.71	34.41	**97.14**
HEPASS algorithm	**4.52**	**94.86**	**3.65**	**97.14**

4 Discussion and conclusion

The diagnostic workload of transplant pathology, which includes donor graft evaluation, transplant follow-up and post-mortem organ assessment can possibly be decreased by implementation of digital algorithms, also known as computer-aided diagnosis.

In this study, we presented a fully automated method for quantitative steatosis assessment in histological images from liver biopsies. Steatotic hepatocytes detection in histological images is a challenging task because of steatosis variability in shape, intensity, and dimension. Our technique did not require any user interaction and it

was capable of automatically detecting steatosis in images with different staining intensity. The proposed method was developed and tested on 385 H&E stained images of liver tissue and automatic results were compared with manual annotations of two expert pathologists. The algorithm showed a very high accuracy during the discrimination between steatosis and non-steatotic tissue (Table 2). Compared with the current state-of-art techniques, our approach achieved the lowest absolute error (around 1%) in the estimation of steatosis percentage (Table 3). In the TEST set, the maximum absolute error of the algorithm was only 5.62%, about 4 times lower respect to compared methods. Finally, the HEPASS algorithm also allowed an improvement of the $SQ_{ACCURACY}$ up to 51.43% compared to previously published methods (Table 4).

The high performances of the HEPASS algorithm were mainly due to the combination of accurate object detection (raw and extended steatosis detection) with semantic segmentation of a deep neural network (cleaning steps). This hybrid approach had the advantage of providing well-defined steatosis contours, with a better delimitation of even small-size macrovesicles. Most of the current state-of-art methods used low-magnification images (x10 or worse) to assess the steatotic hepatocytes, completely neglecting microsteatosis evaluation, which is exceedingly important during liver graft assessment [44]. In addition, our method considered only shape features for selecting the areas of lipid infiltration, avoiding all the error that may occur when chromatic characteristics are used. The main limitation of the HEPASS algorithm is related to the quantification of micro-steatosis. As can be seen from Fig. 6, the absolute error (AE) for micro-steatosis is higher respect to the one related to macro-steatosis. The detection of micro-lipids is even more challenging compared to macro-steatosis as they can have different shapes and intensities. For this reason, we are planning to develop a deep network specifically designed for the detection of micro fat droplets.

To the best of our knowledge, the proposed method is the first fully automated algorithm for the assessment of both micro- and macrosteatosis in H&E stained liver tissue images. The HEPASS algorithm can also be applied to other staining methods (e.g. PAS, trichrome, etc.) as long as steatosis appears as uncolored regions.

The algorithm can be also employed in other fields of hepatic pathology, like discrimination of non-alcoholic steatohepatitis (NASH) versus non-alcoholic fatty liver disease (NAFLD), which present similar morphological features and require the use of dedicated check-list for steatosis quantification and grading [23]. Fig. 7 shows the application of the HEPASS algorithm on a whole-slide image (WSI). The use of automated algorithms may provide more consistent case evaluation guaranteeing quality control, potentially reducing the requirement for high number of expert pathologists. Moreover, digital dataset being uploaded and available on centralized platform may be of use of educational and training purposes, overcoming logistical obstacles.

alt-text: Fig. 7

Fig. 7

Figure Replacement Requested
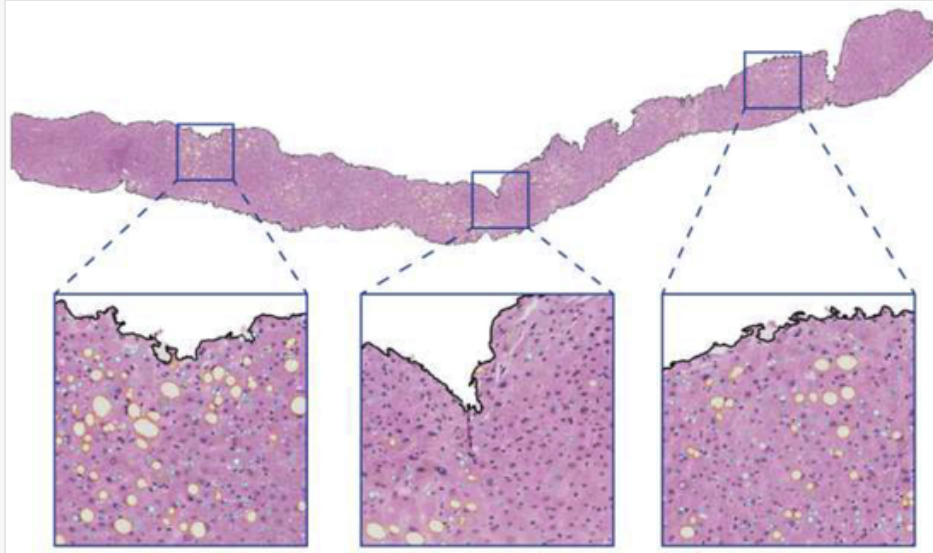
Result of HEPASS processing on a whole-slide image. Tissue boundaries are highlighted in black while macro- and micro steatosis are shown in orange and cyan, respectively. ~~(For interpretation of the references to color in this figure legend, the reader is referred to the Web version of this article.)~~

Replacement Image: Figure 7.tif

Replacement Instruction: High-quality image

In conclusion, we have developed a novel algorithm that enables a fully automated steatosis proportionate area (SPA) assessment, which could be used in human liver grafts evaluation, and it may help to standardize the SQ among pathologists and different centers, and possibly decrease the workload in the routine practice. Being very fast (average computational time: 0.72 s), this method has also the potential to be incorporated into real-time liver graft assessments with frozen liver slides to ensure optimal utilization of the liver graft pool. Our group is currently working on an extension of this algorithm for the processing of entire liver biopsies, with the aim to extract morphological/spatial parameters and find the clinicopathological correlations between the severity of steatosis and patient outcomes.

Declaration of competing interest

We declare that we do not have any commercial or associative interest that represents a conflict of interest in connection with the work submitted.

Acknowledgment

Fedele e Ms. Francesca Veneziano of the Division of Pathology (A. O. U. Città della Salute e della Scienza Hospital, Turin, Italy) that assisted in digitalizing histological slides.

Appendix A Supplementary data

Abbreviations

HEPASS	HEPatic Adaptive Steatosis Segmentation
H&E	Hematoxylin and Eosin
LT	Liver transplantation
EDC	Extended donor criteria
SPA	Steatosis proportionate area
TP	True positive
TN	True negative
FN	False negative
FP	False positive
AE	Absolute error
SQ	Steatosis quantification

References

ⓘ The corrections made in this section will be reviewed and approved by a journal production editor. The newly added/removed references and its citations will be reordered and rearranged by the production team.

[1] Wertheim J.A., Petrowsky H., Saab S., Kupiec-Weglinski J.W., Busuttil R.W., Major challenges limiting liver transplantation in the United States, Am. J. Transplant. 11 (2011) 1773–1784.

[2] Trotter J.F., Liver transplantation around the world, Curr. Opin. Organ Transplant. 22 (2017) 123–127.

[3] Rao K.V., Anderson W.R., Kasiske B.L., Dahl D.C., Value of liver biopsy in the evaluation and management of chronic liver disease in renal transplant recipients, Am. J. Med. 94 (1993) 241–250.

[4] Yan Z., Zhang S., Tan C., Qin H., Belaroussi B., Yu H.J., Miller C., Metaxas D.N., Atlas-based liver segmentation and hepatic fat-fraction assessment for clinical trials, Comput. Med. Imag. Graph. 41 (2015) 80–92.

[5] Alkofer B., Samstein B., V Guarrera J., Kin C., Jan D., Bellemare S., Kinkhabwala M., Brown R., Emond J.C., Renz J.F., Extended-donor criteria liver allografts Seventh Avenue, Semin. Liver Dis., Copyright©, 333, Thieme Medical Publishers, Inc., New, 2006, pp. 221–233 2006.

[6] Busuttil R.W., Tanaka K., The utility of marginal donors in liver transplantation, Liver Transplant. 9 (2003) 651–663.

[7] Mihaylov P., Mangus R., Ekser B., Cabrales A., Timsina L., Fridell J., Lacerda M., Ghabril M., Nephew L., Chalasani N., Expanding the Donor Pool with Utilization of Extended Criteria DCD Livers, Liver Transplant. (2019) 1198–1208.

[8] Soejima Y., Shimada M., Suehiro T., Kishikawa K., Yoshizumi T., Hashimoto K., Minagawa R., Hiroshige S., Terashi T., Ninomiya M., Use of steatotic graft in living-donor liver transplantation, Transplantation 76 (2003) 344–348.

[9] Salizzoni M., Franchello A., Zamboni F., Ricchiuti A., Cocchis D., Fop F., Brunati A., Cerutti E., Marginal grafts: finding the correct treatment for fatty livers, Transpl. Int. 16 (2003) 486–493.

[10] McCormack L., Dutkowski P., El-Badry A.M., Clavien P.-A., Liver transplantation using fatty livers: always feasible?, J. Hepatol. 54 (2011) 1055–1062.

[11] Deschenes M., Early allograft dysfunction: causes, recognition, and management, Liver Transplant. 19 (2013) S6–S8.

[12] Nocito A., El-Badry A.M., Clavien P.-A., When is steatosis too much for transplantation?, J. Hepatol. 45 (2006) 494–499.

[13] Ploeg R.J., D'Alessandro A.M., Knechtle S.J., Stegall M.D., Pirsch J.D., Hoffmann R.M., Sasaki T., Sollinger H.W., Belzer F.O., Kalayoglu M., Risk factors for primary dysfunction after liver transplantation--a multivariate analysis, Transplantation 55 (1993) 807–813.

[14] Angele M.K., Rentsch M., Hartl W.H., Wittmann B., Graeb C., Jauch K.W., Loehe F., Effect of graft steatosis on liver function and organ survival after liver transplantation, Am. J. Surg. 195 (2008) 214–220.

[15] Attia M., Silva M.A., Mirza D.F., The marginal liver donor–an update, Transpl. Int. 21 (2008) 713–724.

[16] de Graaf E.L., Kench J., Dilworth P., Shackel N.A., Strasser S.I., Joseph D., Pless H., Crawford M., McCaughan G.W., Verran D.J., Grade of deceased donor liver macrovesicular steatosis impacts graft and recipient outcomes more than the Donor Risk Index, J. Gastroenterol. Hepatol. 27 (2012) 540–546.

[17] Andert A., Ulmer T.F., Schöning W., Kroy D., Hein M., Alizai P.H., Heidenhain C., Neumann U., Schmeding M., Grade of donor liver microvesicular steatosis does not affect the postoperative outcome after liver transplantation, Hepatobiliary Pancreat, Dis. Int. 16 (2017) 617–623.

[18] Ahmed E.A., El-Badry A.M., Mocchegiani F., Montalti R., Hassan A.E.A., Redwan A.A., Vivarelli M., Impact of graft steatosis on postoperative complications after liver transplantation, Surg. J. 4 (2018) e188 –e196.

[19] Wong T.C.L., Fung J.Y.Y., Chok K.S.H., Cheung T.T., Chan A.C.Y., Sharr W.W., Dai W.C., Chan S.C., Lo C.M., Excellent outcomes of liver transplantation using severely steatotic grafts from brain-dead donors, Liver Transplant. 22 (2016) 226–236.

[20] Brunt E.M., Nonalcoholic steatohepatitis: definition and pathology, Semin. Liver Dis., Copyright© 2001 by Thieme, 333, Medical Publishers, Inc., New, 2001, pp. 3–16 Seventh Avenue.

[21] Hall A.R., Dhillon A.P., Green A.C., Ferrell L., Crawford J.M., Alves V., Balabaud C., Bhathal P., Bioulac-Sage P., Guido M., Hepatic steatosis estimated microscopically versus digital image analysis, Liver Int. 33 (2013) 926–935.

[22] El-Badry A.M., Breitenstein S., Jochum W., Washington K., Paradis V., Rubbia-Brandt L., Puhan M.A., Slankamenac K., Graf R., Clavien P.-A., Assessment of hepatic steatosis by expert pathologists: the end of a gold standard, Ann. Surg. 250 (2009) 691–697.

[23] Kleiner D.E., Brunt E.M., Van Natta M., Behling C., Contos M.J., Cummings O.W., Ferrell L.D., Liu Y., Torbenson M.S., Unalp-Arida A., Design and validation of a histological scoring system for nonalcoholic fatty liver disease, Hepatology 41 (2005) 1313–1321.

[24] Salvi M., Molinari F., Multi-tissue and multi-scale approach for nuclei segmentation in H&E stained images, Biomed. Eng. Online 17 (2018), doi:10.1186/s12938-018-0518-0.

[25] Xu H., Lu C., Berendt R., Jha N., Mandal M., Automated analysis and classification of melanocytic tumor on skin whole slide images, Comput. Med. Imag. Graph. 66 (2018) 124–134.

[26] Belhomme P., Toralba S., Plancoulaine B., Oger M., Gurcan M.N., Bor-Angelier C., Heterogeneity assessment of histological tissue sections in whole slide images, Comput. Med. Imag. Graph. 42 (2015) 51–55.

[27] Batool N., Detection and spatial analysis of hepatic steatosis in histopathology images using sparse linear models, Sixth Int. Conf. Image Process. Theory, Tools Appl., IEEE, 2016, pp. 1–6 2016.

[28] Vanderbeck S., Bockhorst J., Komorowski R., Kleiner D.E., Gawrieh S., Automatic classification of white regions in liver biopsies by supervised machine learning, Hum. Pathol. 45 (2014) 785–792.

[29] Catta-Preta M., Mendonca L.S., Fraulob-Aquino J., Aguila M.B., Mandarim-de-Lacerda C.A., A critical analysis of three quantitative methods of assessment of hepatic steatosis in liver biopsies, Virchows Arch. 459 (2011) 477.

[30] Turlin B., Ramm G.A., Purdie D.M., Lainé F., Perrin M., Deugnier Y., Macdonald G.A., Assessment of hepatic steatosis: comparison of quantitative and semiquantitative methods in 108 liver biopsies, Liver Int. 29 (2009) 530–535.

[31] Liquori G.E., Calamita G., Cascella D., Mastrodonato M., Portincasa P., Ferri D., An innovative methodology for the automated morphometric and quantitative estimation of liver steatosis, Histol. Histopathol. (2009) 41–60.

[32] Tsiplakidou M., Tsipouras M., Giannakeas N., Tzallas A., Manousou P., Automated detection of liver histopathological findings based on biopsy image processing, Information 8 (2017) 36.

[33] Nativ N.I., Chen A.I., Yarmush G., Henry S.D., Lefkowitch J.H., Klein K.M., Maguire T.J., Schloss R., V Guarrera J., Berthiaume F., Automated image analysis method for detecting and quantifying macrovesicular steatosis in hematoxylin and eosin–stained histology images of human livers, Liver Transplant. 20 (2014) 228–236.

[34]

Munsterman I.D., Van Erp M., Weijers G., Bronkhorst C., de Korte C.L., Drenth J.P.H., van der Laak J.A.W.M., Tjwa E.T.T.L., A novel automatic digital algorithm that accurately quantifies steatosis in NAFLD on histopathological whole-slide images, Cytometry B Clin. Cytometry (2019) 521–528.

[35] Arjmand A., Giannakeas N., Fat quantitation in liver biopsies using a pretrained classification based system, Eng. Technol. Appl. Sci. Res. 8 (2018) 3550–3555.

[36] Bala R., Eschbach R., Spatial color-to-grayscale transform preserving chrominance edge information, Color Imaging Conf, Society for Imaging Science and Technology, 2004, pp. 82–86.

[37] Otsu N., A threshold selection method from gray-level histograms, IEEE Trans. Syst. Man. Cybern. 9 (1979) 62–66.

[38] Salvi M., Molinari F., Dogliani N., Bosco M., Automatic discrimination of neoplastic epithelium and stromal response in breast carcinoma, Comput. Biol. Med. 110 (2019) 8–14, doi:10.1016/j.compbiomed.2019.05.009.

[39] Salvi M., Michielli N., Molinari F., Stain Color Adaptive Normalization (SCAN) algorithm: separation and standardization of histological stains in digital pathology, Comput. Methods Progr. Biomed. (2020) 105506.

[40] Chan T.F., Vese L.A., Active contours without edges, IEEE Trans. Image Process. 10 (2001) 266–277.

[41] He K., Zhang X., Ren S., Sun J., Deep residual learning for image recognition, Proc. IEEE Conf. Comput. Vis. Pattern Recognit., 2016, pp. 770–778.

[42] Krizhevsky A., Sutskever I., Hinton G.E., Imagenet classification with deep convolutional neural networks, Adv. Neural Inf. Process. Syst. (2012) 1097–1105.

[43] Rebouças Filho P.P., Cortez P.C., da Silva Barros A.C., De Albuquerque V.H.C., Novel Adaptive Balloon Active Contour Method based on internal force for image segmentation–A systematic evaluation on synthetic and real images, Expert Syst. Appl. 41 (2014) 7707–7721.

[44] Sherlock S., Dooley J., Diseases of the Liver and Biliary System, Wiley Online Library, 2002

Highlights

- Liver steatosis has an important role in assessing the suitability for transplant.

- Histological assessment is subjected to inter- and intra-observer variability.

- An automated method is presented to detect both the micro- and macrosteatosis.

- An accuracy of 97.53% and 97.27% was achieved in train and test set, respectively.

- The algorithm paves the way for quantitative and real-time liver graft assessments.